Finite Element Simulations and Corresponding Experiments of An Advanced Low-Speed High-Torque Permanent Magnet Vernier In-Wheel Motor for Electric Vehicles

Jiangui Li, K.T. Chau
Department of Electrical and Electronic Engineering
The University of Hong Kong, Hong Kong
jgli@eee.hku.hk

Abstract — Vernier machine has been known as a promising candidate for low-speed high-torque applications, because they can provide high-frequency inner-stator operation and low-speed outer-rotor design. A new in-wheel permanent-magnet vernier (PMV) machine has been proposed in this paper. The finite element method is used to analyze the harmonics of the key factors. The proposed PMV in-wheel motor has been prototyped for experimentation. The simulation results agree well with experimental results. The study showcases that the proposed in-wheel motor can offer high torque, which is highly desirable and meaningful for EVs. Detailed simulation and experimental results will be given in the full paper.

I. Introduction

In-wheel motors are becoming attractive for electric vehicles (EVs), since they can provide the direct-drive capability and the feature of electronic differential. As present, the in-wheel motor is based on either a low-frequency low-speed gearless outer-rotor motor or a high-frequency high-speed planetary-geared inner-rotor motor [1]. The former one suffers from the disadvantage of bulky size and heavy weight, while the latter one inevitably involves transmission loss, acoustic noise and regular lubrication. Recently, the coaxial magnetic gear was proposed to solve the problem of planetary gear [2]-[4]. However, the magnetic-geared in-wheel motor still suffers from the drawback of complexity which involves three concentric airgaps. On the other hand, by using the magnetic hearing effect, the permanent magnet vernier (PMV) machine was developed to offer low-speed high-torque rotation [5]-[7]. In this paper, the concept of PMV machine is extended to in-wheel motors. Hence, a new PMV in-wheel motor, having high-frequency inner-stator operation and low-speed outer-rotor rotation, is proposed and implemented for EVs.

II. Theoretical Analysis

The proposed PMV in-wheel motor is shown in Fig. 1, in which the inner stator adopts high-frequency machine design, and the outer rotor is directly mounted with the tire. The key is to incorporate the flux-modulation poles (FMPs) which modulate the high-speed rotating field of the armature windings and the low-speed rotating field of the outer rotor. A group of analytical equations concerning the airgap flux density, the magnetic motive force and the torque are evaluated considering the harmonics to describe the behavior of the proposed machine. The detailed equations will be given in the full paper considering the limited space of the abstracts.

$$\begin{aligned} B_{PM} &\approx F_{PM1}\cos[Z_2(\theta_1-\theta_m)][P_0+P_1\cos(Z_1\theta_1)] \\ &\approx B_{PMh}\cos[Z_2(\theta_1-\theta_m)]+\frac{1}{2}B_{PM1}\cos[(Z_2-Z_1)\theta_1-Z_2\theta_m] \end{aligned} \tag{1}$$

$$T=\frac{p\lambda l}{\pi}\int_0^{2\pi}[P(F_c+F_{PM})]\frac{\partial F_{PM}}{\partial \theta_m}d\theta_1 \tag{2}$$

III. Simulation Results And Experimental Verification

The knowledge of the field distribution in the airgap of the PMV is vitally important for predicting and optimizing its performances [8]. The flux distribution of the proposed machine at 0° and 90° electric degree corresponding to the rotor at the initial position and one fourth of the pole pitch, are shown in Fig. 2. It can be observed that the flux lines per stator tooth can pass through the FMPs separately and they are forced to pass through the rotor iron and the FMPs in an alternate manner, hence verifying the desired flux modulation. The corresponding airgap flux density and its harmonic spectra are shown in Fig. 3. It can be seen that the flux density has 24 pole-pairs in the airgap within 360°, agreeing well with the number of PM pole-pairs. It can also be noted that the order corresponding to 24 pole-pairs has the largest value. There are also several other orders have significant values and should be further studied. The data of the proposed machine is shown in TABLE I.

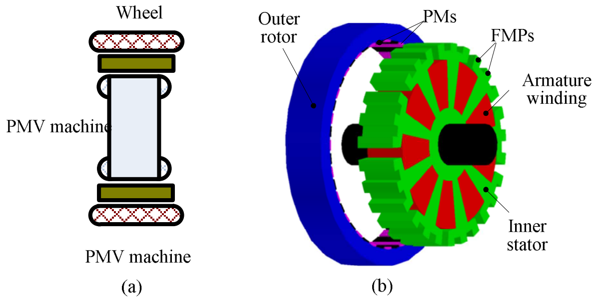

Fig. 1. Proposed PMV machine. (a) In-wheel system. (b) Scheme.

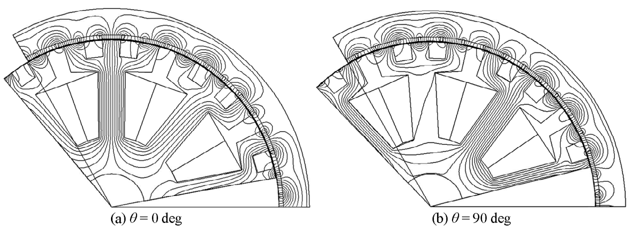

Fig. 2. Flux distribution. (a) At 0°. (b) At 90°.

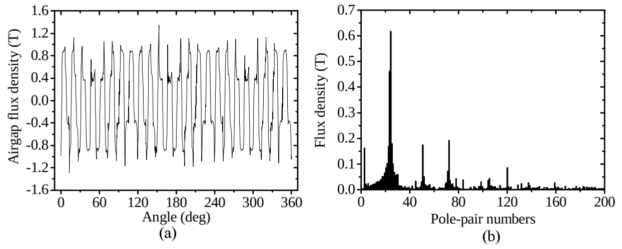

Fig. 3. Airgap flux density. (a) Waveform. (b) Harmonic spectra.

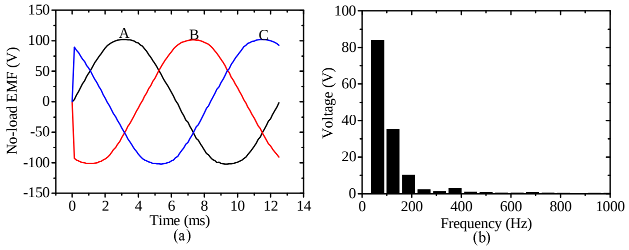

Fig. 4. No-load EMF. (a) Waveform. (b) Harmonic spectra.

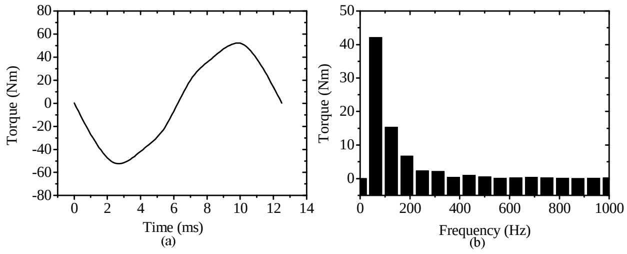

Fig. 5. Torque and harmonic spectra. (a) Waveform. (b) Harmonic spectra.

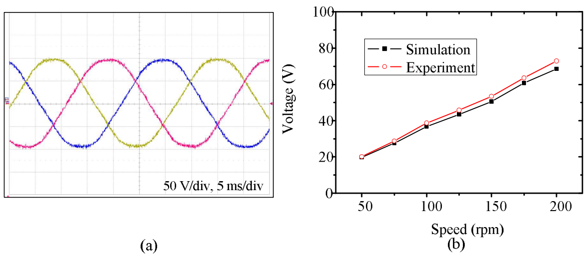

Fig. 6. Measured no-load EMF. (a) Measured at 200 rpm. (b) No-load EMF vs. speed.

The no-load electromotive force (EMF) waveforms are shown in Fig. 4. The no-load EMF waveforms are very sinusoidal which is desirable for smooth torque production. Then, the electromagnetic torque waveform and its harmonic spectrum are obtained under the locked-rotor operation as described in Fig. 5.

Furthermore, the proposed PMV in-wheel motor has been prototyped for experimentation. The measured no-load EMF waveforms and the corresponding voltage versus speed characteristic are shown in Fig. 6. It can be found that the measured results agree well with the simulation results. The detailed simulation and experimental results will be given in the full paper.

TABLE I
DESIGN DATA

Item	Parameter
Rated Power	2 kW
Rated Speed	200 rpm
Overall outside diameter	240 mm
Shaft diameter	40 mm
Axial length	60 mm
Airgap length	0.6 mm
No. of stator pole-pairs	3
No. of stator slots	27
No. of rotor pole-pairs	8

ACKNOWLEDGMENT

This work was supported by a grant (Project No. HKU7105/07E) from the Hong Kong Research Grants Council, Hong Kong Special Administrative Region, China.

IV. CONCLUSION

Vernier machine has been known as a promising candidate for low-speed high-torque applications. Although its principle of operation is resemble to the class of harmonic machines, the corresponding analyses are generally based on the use of fundamental component only while the harmonic components are ignored. In fact, some harmonics of the airgap flux density are significant which should not be neglected. In this paper, the detailed working principle and the performances of the new PMV machine hav been analyzed by an analytical approach, finite element method and experimentation. The analytical analysis results agree well with those obtained by the finite element method and experimental results. The detailed simulation and experimental results will be given in the full paper.

V. REFERENCES

[1] L. Jian, K. T. Chau, Y. Gong, C. Yu and W. L. Li, "Analytical calculation of magnetic field in surface-inset permanent magnet motors," *IEEE Trans. on Magn.*, vol. 45, no. 10, 2009, pp. 4688-4691.

[2] K. Atallah and D. Howe, "A novel high-performance magnetic gear," *IEEE Trans. on Magn.*, vol. 37, no. 4, 2001, pp. 2844-2846.

[3] K. T. Chau, D. Zhang, J. Z. Jiang, C. H. Liu, and Y. J. Zhang, "Design of a magnetic-geared outer-rotor permanent-magnet brushless motor for electric vehicles," *IEEE Trans. on Magn.*, vol. 43, no. 6, 2007, pp. 2504-2506.

[4] P. O. Rasmussen, T. O. Andersen, F. T. Jorgensen, and O. Nielsen, "Development of a high-performance magnetic gear," *IEEE Trans. on Industry Appl.*, vol. 41, no. 3, 2005, pp. 764-770.

[5] J. G. Li, K.T. Chau, J. Z. Jiang, C. H. Liu and W. L. Li, "A new efficient permanent-magnet vernier machine for wind power generation," *IEEE Trans. on Magn.*, vol. 45, no. 6, 2010, pp. 1475-1478.

[6] A. Toba, and T. A. Lipo, "Generic torque-maximizing design methodology of surface permanent-magnet vernier machine," *IEEE Trans. on Industry Appl.*, vol. 36, no. 6, 2000, pp. 1539-1546.

[7] E. Spooner and L. Haydock, "Vernier hybrid machines," *IEE Proc. of Elec. Power Appl.*, vol. 150, no. 6, 2003, pp. 655-662.

[8] Z. Q. Zhu and D. Howe, "Instantaneous magnetic field distribution in brushless permanent magnet dc motors, Part III: Effect of stator slotting," *IEEE Trans. on Magn.*, vol. 29, no. 1, 1993, pp. 143-151.